Proc. Indian Acad. Sci. (Earth Planet. Sci.), Vol. 103, No. 2, June 1994, pp. 163–176.
© Printed in India.

A model study of seasonal mixed-layer primary production in the Arabian Sea

JOHN BROCK[1], SHUBHA SATHYENDRANATH[2,1] and TREVOR PLATT[1]

[1]Biological Oceanography Division, Bedford Institute of Oceanography, Box 1006, Dartmouth, Nova Scotia, Canada B2Y 4A2.
[2]Department of Oceanography, Dalhousie University, Halifax, Nova Scotia, Canada B3H 4J1.

Abstract. We combined a surface irradiance model with a non-spectral photosynthesis-irradiance model to estimate the daily, average rate of mixed-layer primary production in the Arabian Sea for the 15th day of months at the end of the northeast monsoon, the southwest monsoon, and the fall and spring inter-monsoons. Our model experiment uses climatologies of cloud cover, mixed-layer thickness, and satellite ocean-color observations of phytoplankton biomass.

Modelled surface radiation is at an annual maximum in May beneath nearly cloud-free skies just prior to the summer solstice. The model estimate of surface radiation diminishes through the southwest monsoon over most of the northern Arabian Sea to an annual minimum in August due to intense cloudiness.

In agreement with previous ship-based measurements, the photosynthesis-irradiance model predicts that the mixed-layer primary production in the Arabian Sea is extremely seasonal, and peaks annually during the southwest monsoon to the north-west of the atmospheric Findlater Jet and along the coast of Somalia. Northern Arabian Sea maxima predicted for both the summer and winter monsoons are separated by periods of low mixed-layer primary production, the fall and spring inter-monsoons. The annual cycles of modelled mixed-layer primary production differ by region in the Arabian Sea due to varying monsoon influence and circulation dynamics.

Keywords. Arabian Sea; primary production; photosynthesis-light model.

1. Introduction

The monsoon climate of the north-western Indian Ocean, or Arabian Sea, drives a striking semi-annual reversal of surface currents, one of the world's foremost examples of wind-driven ocean circulation (Wyrtki 1973). Forced by surface low-level south-easterly from the southern hemisphere in June through September, the vigorous and deep anticyclonic circulation of the southwest monsoon is typically at peak strength in July and August (Wyrtki 1973; Schott 1983; Swallow 1984; Luther *et al* 1985). The northeast monsoon, generally from December through February, is marked by a westward flow in the Arabian Sea that collapses with the onset of spring. During the periods of wind transition, the fall and spring inter-monsoons, surface currents dissipate and the shallow hydrography approaches that of an unperturbed tropical ocean (Babenerd and Krey 1974; Hastenrath and Greischar 1989; Brock *et al* 1993).

Intense seasonal variations in primary production have been observed in the Arabian Sea (Ryther *et al* 1966; Kabanova 1968; Radhakrishna *et al* 1978; Smith 1984). The primary production in the basin peaks during the southwest monsoon due to upwelling that yields high concentrations of nutrients at shallow depths within

the euphotic zone (Ryther and Menzel 1965; Ryther *et al* 1966; Kuz'menko 1977). Primary production has been observed to exceed $1000\,mg\,Cm^{-2}\,d^{-1}$ during the southwest monsoon and $500\,mg\,Cm^{-2}\,d^{-1}$ during the northeast monsoon over most of the northern Arabian Sea (Kabanova 1968). Extremes in primary production observed for the monsoons alternate with oligotrophic transition seasons in fall and spring (Babenerd and Krey 1974; Krey and Babenerd 1976).

The purpose of this paper is to use surface light and photosynthesis-irradiance models to estimate seasonal changes in the mixed-layer primary production of the Arabian Sea. The objectives are to: (1) assess monthly mean surface shortwave radiation, (2) estimate the primary production of the mixed-layer for months that represent the four seasons of the Arabian Sea, and thereby (3) account for the peaks in primary production observed in ship-based measurements during the monsoons.

Parametrising the most complex primary production models requires description of the vertical chlorophyll profile, the wavelength and angular structure of the submarine light field, and a non-linear, spectrally sensitive photosynthesis-light curve (the $P-I$ curve) (Platt *et al* 1991). For these complex models, extrapolation of a local algorithm to basin-scale requires knowledge of the temporal and spatial variation of these parametres, which could be based on a seasonally-dynamic partitioning of the basin into biogeochemical provinces (Platt and Sathyendranath 1988).

Given that rigorous biogeochemical classification of the Arabian Sea would be premature at present, we have allowed certain simplifications to enable an initial model investigation of the primary production in the Arabian Sea. We have restricted our model experiment to the mixed-layer, which is assumed to have vertically uniform phytoplankton biomass, and have ignored spectral dependencies and effects due to the angular distribution of submarine light. Further, these simplifications allow the use of a computationally rapid polynomial approximation to the exact solution for daily integral of photosynthesis (Platt *et al* 1990; Platt and Sathyendranath 1991).

For highly productive areas of the Arabian Sea undergoing active monsoonal upwelling, the estimate of mixed-layer production should be close to the total, water-column primary production: according to a previous submarine light model experiment (Brock *et al* 1993), during such periods the euphotic zone is shallower than the mixed-layer, which implies that production from below the mixed-layer is negligible. Thus, in the Arabian Sea, the vertical chlorophyll profile can be assumed uniform, and depths below that of the mixed-layer may be ignored, for estimating total, water-column primary production within monsoonal phytoplankton blooms. Although total primary production is quite low during the inter-monsoon periods in spring and fall, or during the monsoons outside eutrophic regions, Brock *et al* (1993) suggest that in such cases an important fraction of the production comes from below the mixed-layer. For these situations, a non-uniform vertical chlorophyll profile that includes a subsurface maximum is required for accurate estimates of total, water-column production. Therefore, the computed mixed-layer production during the inter-monsoons should not be interpreted as water-column production; the latter can be significantly greater than the former.

2. Approach

The non-spectral photosynthesis-irradiance model of Platt *et al* (1990) and Platt and Sathyendranath (1991) was used to estimate mixed-layer primary production on a

1° grid over the entire Arabian Sea (0°–28°N, 45°–80°E) for the 15th day of four months considered to best represent the hydrographic conditions at the close of each season. These four seasons are the fall inter-monsoon (September – November), the northeast monsoon (December – February), the spring inter-monsoon (March – May), and the southwest monsoon (June – August). Unlike some other definitions of seasons in the Arabian Sea (Webster 1987; Schott *et al.* 1990), these designations are based on the mean oceanographic conditions rather than the timing of wind reversals.

We used a polynomial approximation to the analytic solution for the daily rate of mixed-layer primary production ($P_{Z,T}$; mg C m^{-2} d^{-1}) as a function of surface irradiance at local noon (I_0^m; W m^{-2}) (Platt *et al* 1990; Platt and Sathyendranath 1991). When there is no photo-inhibition, this approximation has the form of a truncated polynomial (Platt and Sathyendranath 1991):

$$P_{Z,T} = \left(\frac{BDP_m^B}{\pi K}\right) \sum_{x=1}^{X} \Omega_x \left(\frac{I_0^m}{I_k}\right)^x - \left(\frac{BDP_m^B}{\pi K}\right) \sum_{x=1}^{X} \Omega_x \left(M \frac{I_0^m}{I_k}\right)^x$$

where

B = Phytoplankton biomass, given as the concentration of chlorophyll-*a* (mg Chl m^{-3}),
D = Daylength (h),
P_m^B = Assimilation number, the specific production at saturating light (mg C(mg Chl)$^{-1}$ h^{-1}),
K = Vertical attenuation coefficient for total photosynthetically-active radiation (m^{-1}),
Ω = Weights for fifth-order polynomial fit ($X = 5$) to daily production integral provided by table 2 in Platt *et al* (1990),
I_0^m = Maximum surface irradiance at local noon (W m^{-2}),
I_k = Adaptation parametre of the $P - I$ curve ($I_k = P_m^B/\alpha^B$, where α^B (mg C(mg Chl)$^{-1}$ h^{-1}(W m^{-2})$^{-1}$) is the initial slope of the $P - I$ curve normalised to biomass), and
$M = \exp^{-KZ_m}$ is the optical transmittance of a mixed-layer of height Z_m (dimensionless).

The local noon surface irradiance under cloud-free skies was estimated using the model of Bird (1984). A simple cloud correction was done as in Platt *et al* (1991) using monthly cloud climatology prepared by the Max Planck Institute (Wright 1988) to obtain I_0^m. This procedure was also used to estimate daily average surface shortwave radiation for comparison with previous climatologies. The Hastenrath and Greischar (1989) climatology was used to define monthly mixed-layer thickness (Z_m), and a monthly climatology of phytoplankton biomass (B) was generated by averaging the monthly (Level 3) phytoplankton pigment concentration fields for the overall life of the CZCS, November 1978 through June 1986 (Feldman *et al* 1989; Brock *et al* 1993). In this implementation, the satellite-observed phytoplankton biomass is assumed to represent vertically uniform mixed-layer biomass. The vertical attenuation coefficient (K) was estimated from the chlorophyll concentration assuming Case 1 waters, using the model results of Sathyendranath and Platt (1988). Thus, the estimates of light attenuation in these calculations are based on a fully spectral optical model, even though the photosynthesis-light model used here is non-spectral. Table 1 describes the data sets used in this study.

Unlike the N. Atlantic, there is very little information available on the photosynthetic parametres P_m^B and α^B from the Arabian Sea. In fact, we were obliged to

Table 1. Data sets used.

Variable	Observational basis	Comment
Cloudiness	Climatology based on the COADS data set	Provided by the Max Planck Institut fur Meteorologie (Wright 1988).
Mixed-layer phytoplankton biomass	Coastal Zone Color Scanner data	Based on monthly average fields from NASA/GSFC (Feldman *et al* 1989).
Mixed-layer depth	Subsurface temperature and salinity soundings	Based on the Master Oceanographic Observation Data Set compiled by the Fleet Numerical Oceanography Center, Monterey, CA (Hastenrath and Greischar 1989).

assign values for these parametres in the preliminary calculations presented here. In view of our emphasis on the monsoon periods of peak production, these values were assigned based on an analysis of historical bio-optical profiles acquired in the northern Arabian Sea during winter and summer periods of eutrophication. With these values of the $P-I$ parametres ($\alpha^B = 0{\cdot}1\,\mathrm{mg\,C(mg\,Chl)^{-1}\,h^{-1}(W\,m^{-2})^{-1}}$) and ($P_m^B = 3{\cdot}0\,\mathrm{mg\,C(mg\,Chl)^{-1}\,h^{-1}}$; note that $I_k = P_m^B/\alpha^B$) the estimated primary production within monsoonal phytoplankton blooms falls in the range of observed production values, whereas it over-estimates production during the inter-monsoons. The dependence of photosynthesis on available light in an oligotrophic mixed-layer is likely to differ from that for regions of high nutrient fluxes (Platt *et al* 1992); but in these initial calculations, we have not made allowances for such changes, mainly due to lack of data from the Arabian Sea.

3. Seasonality of light and mixed-layer hydrography

The atmospheric transmittance model implemented here produces an annual cycle of shortwave radiation that is consistent with previous climatologies (Hastenrath and Lamb 1979; Hsiung 1986; Molinari *et al* 1986). The model predicts that, in spite of the approach of the winter solstice, daily average surface radiation in the photosynthetically active region (400–700 nm) increases through the fall inter-monsoon over all of the Arabian Sea except near the Gulf of Aden (figure 1). The predicted surface radiation increases through winter and spring towards the summer solstice. At the close of the spring inter-monsoon in May, the cloud cover is at the yearly minimum, and modelled daily, average surface radiation in the wavelength interval of 400 to 700 nm is at an annual maximum, increasing to the north to exceed $280\,\mathrm{W\,m^{-2}}$ in the Gulf of Oman. Increased cloudiness that accompanies the onset of the southwest monsoon in late May and early June diminishes surface radiation, particularly in the northeastern Arabian Sea. Here, in August, the model predicts an annual minimum in daily, average radiation reaching the surface for anywhere in the Arabian Sea, less than $170\,\mathrm{W\,m^{-2}}$.

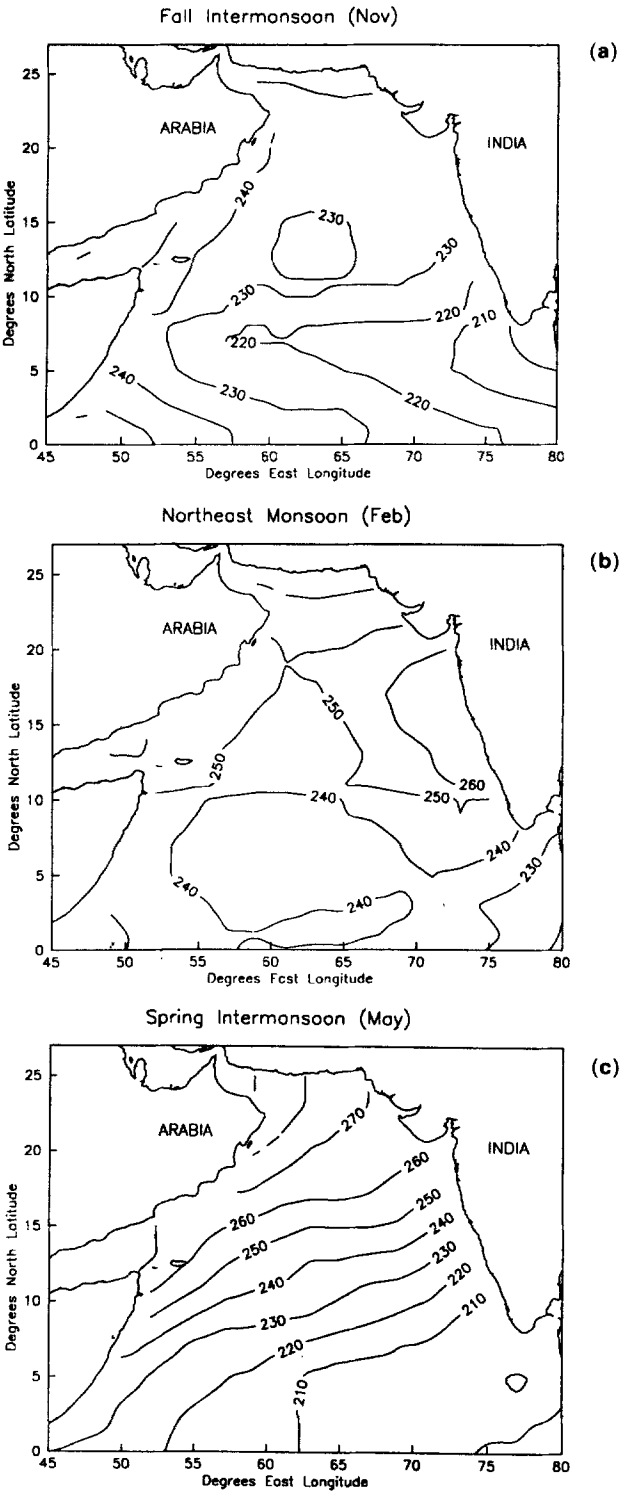
Fall Intermonsoon (Nov)
(a)
ARABIA
INDIA
Degrees North Latitude
Degrees East Longitude
Northeast Monsoon (Feb)
(b)
ARABIA
INDIA
Degrees North Latitude
Degrees East Longitude
Spring Intermonsoon (May)
(c)
ARABIA
INDIA
Degrees North Latitude
Degrees East Longitude

Figure 1.

Figure 1. (*Continued*).

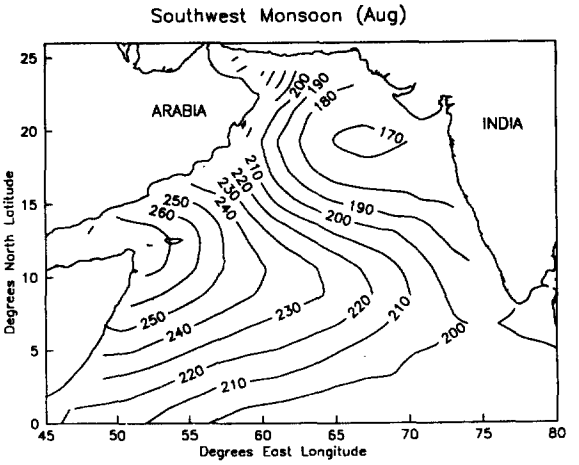

Figure 1. Maps depicting the model estimate of daily average surface shortwave radiation in the photosynthetically active region (400–700 nm) (W m^{-2}) for the 15th day of four months representing the close of each of the four seasons of the Arabian Sea.

High insolation and weak winds (Hastenrath and Greischar 1989) result in a thin, oligotrophic mixed-layer during inter-monsoons in fall and especially in spring (Colburn 1975; Banse 1987; Rao *et al* 1989; Naidu and Rao 1990). In May the mixed-layer in the open Arabian Sea is mostly shoaler than 50 m (Hastenrath and Greischar 1989), and climatological pigment concentrations observed by the CZCS are generally less than 0·1 mg m^{-3} (Feldman *et al* 1989; Brock *et al* 1993). Historical vertical profiles of temperature and phytoplankton pigments (Yentsch 1965; Saijo 1973; Krey and Babenerd 1976; Karabashev and Solov'yev 1978; Hay *et al* in press), ship-observed surface chlorophyll concentrations (Babenerd and Krey 1974; Banse 1987), and mixed-layer depth (Hastenrath and Greischar 1989) and satellite-based phytoplankton biomass climatologies (Feldman *et al* 1989; Brock *et al* 1993) strongly suggest that in May almost the entire Arabian Sea attains the "Typical Tropical Structure" (TTS), first described in the eastern tropical Atlantic (Herbland and Voituriez 1977, 1979). Shoaling of the mixed-layer and a spread of oligotrophy across the basin suggest that following the close of summer monsoon, the Arabian Sea again approaches the TTS, although during the fall inter-monsoon this trend is apparently stunted by the less intense ocean heat gain (Hastenrath and Greischar 1989).

In contrast, both the winter and summer monsoons result in mixed-layer deepening and regional phytoplankton blooms in the Arabian Sea (Banse and McClain 1986; Banse 1987; Hastenrath and Greischar 1989; Bauer *et al* 1991; Brock *et al* 1991; Brock and McClain 1992). Blooms in winter are probably due to vertical mixing caused by wind stirring or convective overturn (Banse and McClain 1986). Upwelling off the coasts of Somali (Schott 1983; Smith and Codispoti 1980; Smith 1984) and Oman (Bruce 1974; Smith and Bottero 1977; Swallow 1984; Bauer *et al* 1991) during the southwest monsoon yields a phytoplankton bloom (Banse 1987; Bauer *et al* 1991; Brock *et al* 1991) that extends over much of the western Arabian Sea in August. The portion of this bloom that extends over 700 km seaward of the Omani shelf has been attributed to upward Ekman pumping driven by strong positive wind stress curl to the north-west of the Findlater Jet (Findlater 1966) axis (Bauer *et al* 1991; Brock

et al 1991; Brock and McClain 1992). Similarly, the deepening of the summer mixed-layer in the central Arabian Sea has been attributed to convergence in the Ekman layer caused by negative wind-stress curl south of the Findlater Jet axis (Naidu and Rao 1990; Bauer *et al* 1991; McCreary and Kundu 1989; Luther *et al* 1990).

4. Seasonality of mixed-layer primary production

The annual cycle of mixed-layer primary production predicted by the model at a site in the north-western Arabian Sea (14°N, 57°E), the region most strongly influenced by the monsoons, includes a massive peak for the southwest monsoon (above $1700\,mg\,C\,m^{-2}\,d^{-1}$) and a secondary maximum for the northeast monsoon (greater than $300\,mg\,C\,m^{-2}\,d^{-1}$) (figures 2 and 3). Modelled mixed-layer primary production sharply diminishes during both inter-monsoons, and in spring it is generally less than $100\,mg\,C\,m^{-2}\,d^{-1}$.

The results of Brock *et al* (1993) on the underwater light field suggest that late in the winter and summer monsoons the euphotic zone is wholly within the mixed-layer of the northern Arabian Sea. This enables comparison of our modelled mixed-layer production to ship-based measurements of total euphotic zone production for the northern Arabian Sea at the close of both monsoons. Although much variability is

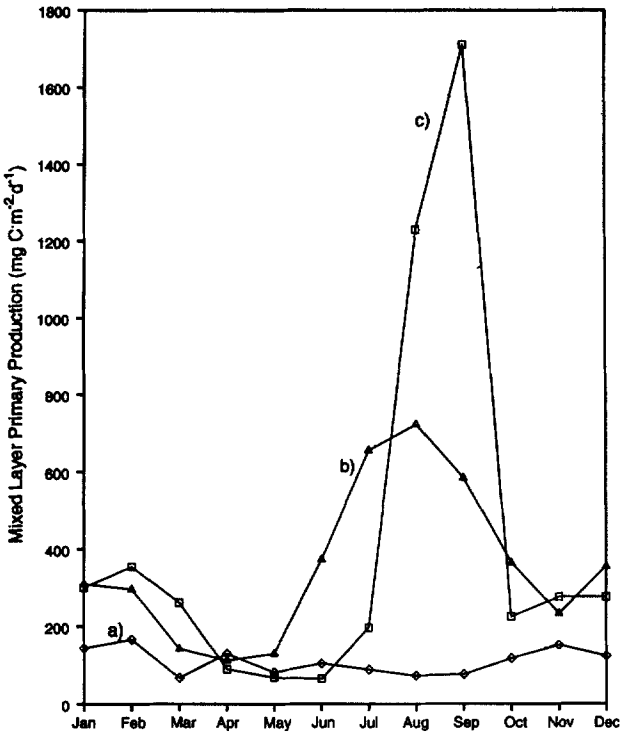

Figure 2. Time series plots of monthly mean daily primary production in the mixed-layer estimated by the model for sites in a) the southeastern Arabian Sea (2°N, 68°E), b) the Somali coast region (10°N, 53°E), and c) the northwestern Arabian Sea (14°N, 57°E).

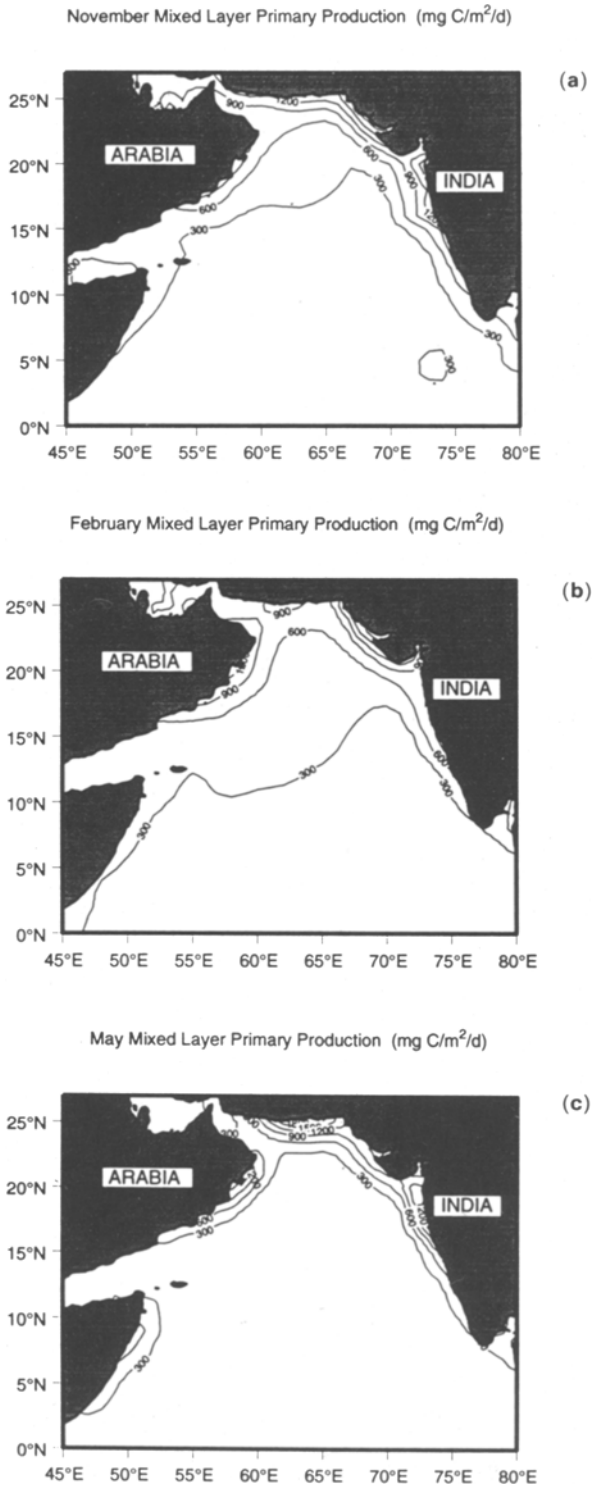
November Mixed Layer Primary Production (mg C/m²/d)
(a)
ARABIA
INDIA
25°N
20°N
15°N
10°N
5°N
0°N
45°E 50°E 55°E 60°E 65°E 70°E 75°E 80°E
February Mixed Layer Primary Production (mg C/m²/d)
(b)
ARABIA
INDIA
25°N
20°N
15°N
10°N
5°N
0°N
45°E 50°E 55°E 60°E 65°E 70°E 75°E 80°E
May Mixed Layer Primary Production (mg C/m²/d)
(c)
ARABIA
INDIA
25°N
20°N
15°N
10°N
5°N
0°N
45°E 50°E 55°E 60°E 65°E 70°E 75°E 80°E

Figure 3.

Figure 3. (*Continued*).

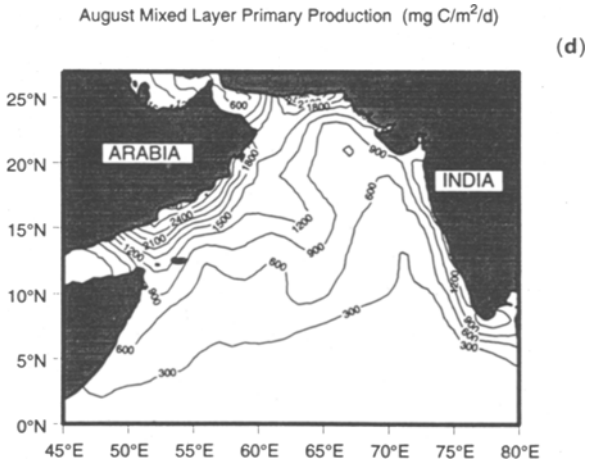

Figure 3. Maps depicting model predictions of daily mixed-layer primary production for the 15th day of months representing the four seasons of the Arabian Sea.

apparent, the disparate ship-based *in situ* and simulated *in situ* measurements of integrated euphotic zone production for the northern Arabian Sea in late winter (Kabanova 1968; Krey 1973) and late summer (Kabanova 1968; Krey 1973; Babenerd and Krey 1974; Qasim 1977) are in general agreement with our model estimates.

This intensely monsoonal cycle of mixed-layer production changes with location in the Arabian Sea, and this regional variation may in future form the basis of a seasonally dynamic biogeochemical classification. In the absence of strong seasonal wind reversals, the annual cycle of mixed-layer production for much of the Arabian Sea would resemble that modelled for its perennially oligotrophic south-eastern portion (figure 2). Here the influence of the monsoons is muted, and the modelled annual pattern is that of a well-stratified and unperturbed tropical ocean, with mixed-layer production consistently less than 200 mg C m^{-2} d^{-1}. The thin and oligotrophic mixed-layer that persists year-round in the south-east spreads north and west during the inter-monsoons, and the daily rate of mixed-layer primary production predicted by the model in mid-November and mid-May is generally less than 300 mg C m^{-2} d^{-1} for all but the northernmost Arabian Sea (figure 2). This low mixed-layer primary production is consistent with the attributes of the classic TTS studied by Herbland and Voituriez (1977, 1979) in the eastern tropical Atlantic.

Circulation dynamics are fundamentally different in the southwest monsoon upwellings off Arabia and East Africa, resulting in a variant of the monsoonal cycle of modelled mixed-layer primary production along the Somali coast (figures 2 and 3). Summer upwelling along Somalia is tied to the formation of the swift Somali Current (Wyrtki 1973; Duing *et al* 1980; Swallow 1984; Luther *et al* 1985) and is focused by large anticyclonic gyres (Brown *et al* 1980; Smith and Codispoti 1980; Smith 1984). As a consequence, off Ras Hafun at 10°N, 53°E the summer peak in modelled mixed-layer primary production arrives 1–2 months earlier than the sharper and more extreme peak off Oman at 14°N, 57°E (figure 2). Note, however, that for the fall and winter no profound differences exist in the mixed-layer production estimated by the model for these regions of the western Arabian Sea.

5. Discussion

In this paper, we have presented preliminary computations of mixed-layer primary production in the Arabian Sea, for months representative of the four seasons in that region. These results are by no means meant to be final: our objective was rather to attempt an initial calculation of primary production in the Arabian Sea at the basin scale, using information that is currently available. We hope that such a calculation would help to highlight the weak links, and identify areas where more work is required, if further improvements are to be made.

In climate-change related studies on primary productivity, it would be necessary to estimate year-to-year changes in solar radiation at the sea surface. In this work, we have used a clear-sky model (Bird 1984) combined with a simple cloud correction to compute the photosynthetically-active radiation and total short-wave radiation at the sea surface. We have shown that these results are consistent with climatologies of short-wave radiation that have been published previously (Hastenrath and Lamb 1979; Hsiung 1986; Molinari *et al* 1986). Recently, Bishop and Rossow (1991) have shown that satellite-derived cloud information can be successfully used to compute surface solar radiation at the global scale. It thus appears that this aspect of the problem is now tractable.

In these calculations, we have based our estimates of the attenuation coeffcient on a general light transmission model. For large-scale estimates of the type presented here, we have to rely on satellite data to provide the necessary input, such as phytoplankton biomass. The next generation of ocean-colour satellites, such as the SeaWiFS, with better radiometric and spectral resolution should improve satellite-derived estimates of biomass, especially in case 2 waters. If regional information on optical characteristics specific to the Arabian Sea were available, it would be possible to improve the estimates of attenuation coefficient further by incorporating these characteristics into models of light transmission.

We know that the computations of primary production are very sensitive to the values assigned to the $P-I$ parametres. In this work, we have had to assume constant values for these parametres, for lack of information. This is admittedly an over-simplification, and this is one area where there is a definite need for more information. Even when observations become available, they would have to be extrapolated in space and time, to match the satellite observations. This would, in turn, call for additional information on how the dynamics of the upper ocean (mixing, nutrient supply) affect these characteristics of the phytoplankton population. The extrapolation schemes would have to respect the natural boundaries in the ocean, which would in turn require an understanding of the biogeochemical provinces in the area.

These computations have been confined to the mixed layer. To extend the calculations to the whole water column, we need additional information on the vertical structure of the water column, with respect to biological and optical properties. Clearly, this information cannot be obtained directly from satellite data, and would therefore have to be built from *in situ* observations and perhaps, models. We have shown (Brock *et al* 1993) that this may not be a serious problem when the waters become eutrophic, but it certainly merits attention when the waters become more oligotrophic.

6. Summary

We used the photosynthesis-irradiance model of Platt *et al* (1990, 1991) to estimate the average daily rate of mixed-layer primary production in the Arabian Sea for months at the close of the winter and summer monsoons, and the fall and spring inter-monsoons. The model of Bird (1984) was used to estimate irradiance at local noon in the absence of clouds. The photosynthesis-irradiance model ignores spectral dependencies and effects due to the angular distribution of submarine light, and uses climatologies of cloud cover (Wright 1988), mixed-layer thickness (Hastenrath and Greischar 1989) and satellite ocean color observations of phytoplankton biomass (Feldman *et al* 1989; Brock *et al* 1993). We assumed Case 1 waters, and estimated the vertical attenuation coefficient from the chlorophyll concentration using a spectral model of light penetration (Sathyendranath and Platt 1988).

Our model experiment is consistent with earlier ship-based measurements (Ryther and Menzel 1965; Ryther *et al* 1966; Kabanova 1968; Krey and Babenerd 1976; Kuz'menko 1977; Radhakrishna *et al* 1978; Smith 1984) and wind-driven circulation models (Luther and O'Brien 1985; Bauer *et al* 1991) suggesting that the primary production in the Arabian Sea is extremely seasonal and peaks annually during the southwest monsoon to the north-west of the atmospheric Findlater Jet and along the coast of Somalia. Northern Arabian Sea maxima in both observed (Babenerd and Krey 1974) and modelled mixed layer primary production are separated by oligotrophic transition periods, the fall and spring inter-monsoons.

Modelled surface radiation in the photosynthetically active region (400–700 nm) increases through fall, winter, and spring over most of the Arabian Sea to an annual maximum in May that exceeds 280 $W m^{-2}$ in the north-west beneath nearly cloud-free skies just prior to the summer solstice. The model estimate of surface radiation diminishes at the onset of the southwest monsoon due to an abrupt increase in cloudiness over the north-central and north-eastern Arabian Sea. Here in August the model predicts an annual minimum in light reaching the surface for anywhere in the Arabian Sea, less than 170 $W m^{-2}$.

The annual cycles of mixed-layer primary production predicted by the model at sites off Oman (14°N, 57°E), in the basin's perennially oligotrophic south-east at 2°N 68°E, and off the Somali coast adjacent to Ras Hafun at 10°N, 53°E differ due to varying monsoon influence and circulation dynamics. A massive southwest monsoon peak (greater than 1700 mg C $m^{-2} d^{-1}$) and secondary northeast monsoon peak separated by periods of low mixed-layer primary production for the inter-monsoons are modelled for the site off Oman. This site in the north-western Arabian Sea exemplifies the annual cycle of the most monsoonal portion of the basin.

In contrast, the cycle modelled for 2°N, 68°E is that of an undisturbed tropical ocean, the Arabian Sea in the absence of monsoons. Here the modelled mixed-layer primary production is uniform and low year-round, never exceeding 200 mg C $m^{-2} d^{-1}$. Yet another variant of the paradigmatic monsoonal cycle in mixed-layer primary production was modelled off the Somali coast. Along East Africa, the formation of the swift Somali current in spring initiates coastal upwelling prior to the onset of upward Ekman pumping in the north-west part of the basin. Consequently, off Ras Hafun the southwest monsoon peak in modelled mixed-layer primary production arrives 1 to 2 months earlier than the sharper and more extreme peak off Oman at 14°N, 53°E.

These computations are meant as a first step towards basin-scale computations of mixed-layer primary production in the Arabian Sea. We have identified areas where more work is required, if further improvements are to be made to this type of calculation.

Acknowledgements

J Brock acknowledges support from the Natural Sciences and Engineering Research Council of Canada. The work presented in this paper was supported, in part, by the Office of Naval Research; the National Aeronautics and Space Administration; the European Space Agency; the Department of Fisheries and Oceans, Canada; and the Department of National Defence, Canada. Additional support was provided by the Natural Sciences and Engineering Research Council through Operating Grants to SS and TP. This work was carried out as part of the Canadian contribution to the Joint Global Ocean Flux Study. The authors thank the Nimbus Project at NASA/GSFC and the University of Miami for Coastal Zone Color Scanner data products. We are grateful to Alan Longhurst for all his help with the manuscript.

References

Babenerd B and Krey J 1974 *Indian Ocean: Collected data on Primary Production, Phytoplankton Pigments, and Some Related Factors*; (Germany: Institut fur Meerskunde an der Universitat Kiel)

Banse K 1987 Seasonality of phytoplankton chlorophyll in the central and northern Arabian Sea; *Deep-Sea Res.* **34** 713–723

Banse K and McClain C R 1986 Satellite-observed winter blooms of phytoplankton in the Arabian Sea; *Mar. Ecol. Proress Series* **34** 201–211

Bauer S, Hitchcock G L, Olson D B 1991 Influence of monsoonally-forced Ekman dynamics upon surface layer depth and plankton biomass distribution in the Arabian Sea; *Deep-Sea Res.* **38** 531–553

Bird R E 1984 A simple, solar spectral model for direct-normal and diffuse horizontal irradiance; *Solar Energy* **32** 461–471

Bishop J K B and Rossow W B 1991 Spatial and temporal variability of global surface solar irradiance; *J. Geophys. Res.* **96** 16,839–16,858

Brock J C, McClain C R, Luther M E and Hay W W 1991 The phytoplankton bloom in the northwestern Arabian Sea during the southwest monsoon of 1979; *J. Geophys. Res.* **96** 20,623–20,642

Brock J C and McClain C R 1992 Interannual variability of the southwest monsoon phytoplankton bloom in the northwestern Arabian Sea; *J. Geophys. Res.* **97** 733–750

Brock J C, Sathyendranath S and Platt T 1993 Modelling the seasonality of subsurface light and primary production in the Arabian Sea; *Mar. Ecol. Progress Series* **101** 209–221

Brown O B, Bruce J G and Evans R H 1980 Evolution of sea surface temperature in the Somali Basin during the southwest monsoon of 1979; *Nature (London)* **209** 595–597

Bruce J G 1974 Some details of upwelling off the Somali and Arabian coasts; *J. Mar. Res.* **32** 419–423

Colburn J G 1975 *The Thermal Structure of the Indian Ocean* (Honolulu: University of Hawaii Press) pp. 173

Duing W, Molinari R L and Swallow J C 1980 Somali Current: Evolution of surface flow; *Science* **209** 588–590

Feldman G *et al* 1989 Ocean color: Availability of the global data set; *EOS Transactions, AGU* **70** 634–635

Findlater J 1966 Cross-equatorial jet streams at low level over Kenya; *The Meteorological Magazine* **95** 353–364

Hastenrath S and Lamb P 1979 *Climatic Atlas of the Indian Ocean. Part II: The Oceanic Heat Budget* (University of Wisconsin Press) 109 pp

Hastenrath and Greischar 1989 *Climatic Atlas of the Indian Ocean. Part III: Upper-Ocean Structure* (University of Wisconsin Press) 247 pp

Hay B J, Petzold M and McClain C R 1992 *Pigment assessment in the Arabian Sea comparing satellite data and in-situ water column measurements* (in press)

Herbland A and Voituriez B 1977 Production primaire, nitrate et nitrite dans l'Atlantique tropical, 1-Distribution du nitrate et production primaire; *Cah. ORSTOM, ser. Oceanogr.* **15** 47–56

Herbland A and Voituriez B 1979 Hydrological structure analysis for estimating the primary production in the tropical Atlantic Ocean *J. Mar. Res.* **37** 87–101

Hsiung J 1986 Mean surface energy fluxes over the global ocean *J. Geophys. Res.* **91** 10,585–10,606

Kabanova Y G 1968 Primary production of the northern part of the Indian Ocean; *Oceanology* **8** 214–225

Karabashev G S and Solov'yev A N 1978 Relation between the fluorescence maxima of phytoplankton pigments and the location of the seasonal pycnocline; *Oceanology* **18** 468–471

Krey J 1973 *Primary production in the Indian Ocean I, in The Biology of the Indian Ocean* 1973 (ed.) B Zeitzschel, (New York: Springer-Verlag) pp. 18–36

Krey J and Babenerd B 1976 *Phytoplankton Production Atlas of the International Indian Ocean Expedition* (Institut fur Meereskunde an der Universitat Kiel)

Kuz'menko L V 1977 Distribution of phytoplankton in the Arabian Sea; *Mar. Biol.* **17** 70–74

Luther M E and O'Brien J J 1985 A model of the seasonal circulation of the Arabian Sea forced by observed winds; *Prog. Oceanogr.* **14** 353–385

Luther M E, O'Brien J J and Meng A H 1985 *Morphology of the Somali Current system during the southwest monsoon, in Coupled Ocean-Atmosphere Models* (ed.) J C J Nihoul (Amsterdam: Elsevier Science Publishers B V) pp. 405–437

Luther M E, O'Brien J J and Prell W L 1990 Variability in upwelling fields in the northwestern Indian Ocean; Part 1; Model experiments over the past 18,000 years; *Paleoceanography* **5** 433–445

McCreary J P and Kundu P K 1989 A numerical investigation of sea surface temperature variability in the Arabian Sea; *J. Geophys. Res.* **94** 16,097–16,114

Molinari R L, Festa J F and Marmolejo E 1986 Heat Budget and Climatic Atlas of the Tropical Western Indian Ocean and Arabian Sea During FGGE (1979); *NOAA Tech. Memo. ERL AOML-63, Atlantic Oceanographic and Meteorological Laboratory, Miami*

Naidu V S and Rao G R L 1990 Ekman pumping velocity and depth of surface mixed-layer of the north Indian Ocean during southwest monsoon *Indian J. Mar. Sci.* **19** 257–260

Paltridge G W and Platt C M R 1976 *Radiative Processes in Meteorology and Climatology* (New York: Elsevier) pp. 60–63

Platt T and Sathyendranath S 1988 Oceanic primary production: Estimation by remote sensing at local and regional scales; *Science* **241** 1613–1620

Platt T, Sathyendranath S and Ravindran P 1990 Primary production by phytoplankton: analytic solutions for daily rates per unit area of water surface; *Proc. R. Soc. London* **B241** 101–111

Platt T, Caverhill C and Sathyendranath S 1991 Basin-scale estimates of oceanic primary production by remote sensing: The North Atlantic; *J. Geophys. Res.* **96** 15,147–15,159

Platt T and Sathyendranath S 1991 Biological production models as elements of coupled, atmosphere-ocean models for climate research; *J. Geophys. Res.* **96** 2585–2592

Platt T, Sathyendranath S, Ulloa O, Harrison W G, Hoepffner N and Goes J 1992 Nutrient control of phytoplankton photosynthesis in the western North Atlantic *Nature (London)* **356** 229–231

Qasim S Z 1977 Biological productivity of the Indian Ocean; *Indian J. Mar. Sci.* 122–137

Radhakrishna K, Devassy V P, Bhargava R M S and Bhattathiri P M A 1978 Primary production in the Arabian Sea; *Indian J. Mar. Sci.* **7** 271–275

Rao R R, Molinari R L and Festa J F 1989 Evolution of the climatological near-surface thermal structure of the tropical Indian Ocean. 1. Description of monthly mean mixed-layer depth, and sea surface temperature, surface current, and surface meteorological fields; *J. Geophys. Res.* **94** 10,801–10,815

Ryther J H and Menzel D W 1965 On the production, composition, and distribution of organic matter in the western Arabian Sea; *Deep-Sea Res.* **12** 199–209

Ryther J H, Hall J R, Pease A K, Bakun A and Jones M M 1966 Primary organic production in relation to the chemistry and hydrography of the western Indian Ocean; *Limnol. Oceanogr.* **11** 371–380

Saijo J 1973 *The formation of the chlorophyll maximum in the Indian Ocean, The Biology of the Indian Ocean* (ed.) B Zeitzschel (New York: Springer-Verlag) pp. 171–173

Sathyendranath S and Platt T 1988 The spectral irradiance field at the surface and in the interior of the ocean: A model for applications in oceanography and remote sensing; *J. Geophys. Res.* **93** 9270–9280

Schott F 1983 Monsoon response of the Somali Current and associated upwelling; *Progr. Oceanogr.* **12** 357–381

Schott F, Swallow J C and Fieux M 1990 The Somali Current at the equator: Annual cycle of currents and transports in the upper 1,000 m and connection to neighboring latitudes; *Deep-Sea Res.* **37** 1825–1848

Smith S L 1984 Biological indications of active upwelling in the northwestern Indian Ocean in 1964 and 1979, a comparison with Peru and northwest Africa; *Deep-Sea Res.* **31** 951–967

Smith S L and Codispoti L A 1980 Southwest monsoon of 1979: Chemical and biological response of Somali coastal waters; *Science* **209** 597–600

Smith R L and Bottero J S 1977 *On upwelling in the Arabian Sea, A Voyage of Discovery* (ed.) M Angel (New York: Pergamon Press) pp. 291–304

Swallow J C 1984 Some aspects of the physical oceanography of the Indian Ocean, *Deep-Sea Res.* **31** 639–650

Webster P J 1987 The elementary monsoon; In *Monsoons* (ed.) J S Fein and P L Stephens pp. 3–32, (New York: John Wiley)

Wright P B 1988 An Atlas based on the 'COADS' Data Set: Fields of Mean Wind, Cloudiness and Humidity at the Surface of the Global Ocean; *Report No. 14, Max-Planck-Institut fur Meteorologie, Hamburg*

Wyrtki K 1973 Physical oceanography of the Indian Ocean; In *The Biology of the Indian Ocean* (ed.) B Zeitzschel (New York: Springer-Verlag) pp. 18–36

Yentsch C S 1965 Distribution of chlorophyll and phaeophytin in the open ocean; *Deep-Sea Res.* **12** 653–666